ACCEPTOR AND DONOR-DOPED CARBON NANOTUBES AS ELECTROCATALYSTS FOR ORR, HER AND OER

Paweł SZROEDER[1], Przemysław ZIÓŁKOWSKI[1], Ihor SAHALIANOV[1]

[1]*Kazimierz Wielki University, Faculty of Physics, Bydgoszcz, Poland, EU, psz@ukw.edu.pl*

[2]*Linköping University, Department of Science and Technology, Norrköping, Sweden, EU*

https://doi.org/10.37904/nanocon.2025.5166

Abstract

Pristine carbon nanotubes have relatively weak electrocatalytic activity. On the other hand, due to the symmetry of the π-electron bands, nanotubes can be doped either donor or acceptor to optimize the kinetics of heterogeneous electron transfer. In this report, we focus on analyzing the effects of acceptor (boron), donor (nitrogen) doping and covalent functionalization of nanotubes with -OH group on the electrocatalysis of cathodic oxygen reduction (ORR) and hydrogen evolution reaction (HER), as well as anodic oxygen evolution reaction (OER). Simulations based on the Gerischer-Marcus model show that acceptor doping slightly shifts the onset of ORR and HER reactions to more negative potentials. At the same time, acceptor doping contributes to increasing the efficiency of the anodic OER by significantly reducing reaction overpotential. On the other hand, donor doping remarkably enhances the kinetics of ORR and HER, whose onset potentials are shifted to less negative potentials with respect of pristine CNTs by more than 0.4 V. We also show that covalent functionalization with an -OH group produces an effect analogous to acceptor doping. Experimental data obtained for pristine and hydroxylated CNT electrodes in aqueous 0.1 M KOH solution confirm the predictions of the Gerischer-Marcus model. The results presented outline a strategy for preparing electrode materials containing nanotubes in such applications as fuel cells, metal-air batteries and water splitting.

Keywords: Carbon nanotubes, acceptor doping, donor doping, Gerischer-Marcus model, oxygen reduction reaction, hydrogen evolution reaction, oxygen evolution reaction

1. INTRODUCTION

Carbon nanotubes (CNTs) are one of the most spectacular implementations of one-dimensional π-electron systems, in which efficient charge transport along the nanotube and susceptibility to modification by doping are possible. The unique electronic properties of CNTs enables their potential applications. In particular, carbon nanotubes have been considered as an electrode material in fuel cells [1-3], metal-air batteries [4-6] and electrochemical water splitting [7-10].

The major challenge in the development of fuel cell technology is achieving low-cost non-precious metal ORR electrocatalysts, which characterize with low overpotential of the cathodic reaction and do not degrade. One of the suggested strategies is use of the heteroatom doped nanocarbons [11]. In metal-air batteries, on the other hands, the sluggish kinetics of the ORR/OER stands in the way of achieving satisfactory electrochemical performance [12]. In OER catalysis, the d-bands formed by 3d transition metal elements play an important role in influencing the strength of adsorption of reagents and intermediates. Currently, mainstream research focuses on high-entropy alloys containing, among others, Co, Ni, Cr, Mn, V, Ti, Fe, in which the position of the d-band center can be optimized by changing the content of the components [13]. Nevertheless, it has been shown that nanoparticles of transition metal alloys encapsulated in N-doped carbon nanotubes exhibit improved catalytic performance and lifetime [14]. The electrochemical water splitting involves OER at the anode and HER at the anode. The benchmark catalysts for the HER is Pt/C owing to their moderate chemical

bond strength with reaction intermediates. In general, 3d transition metals are widely recognized as HER catalysts [15]. In particular, it has been shown that deposition of single atoms of vanadium on C_{60} results in decreasing the energy barrier of the HER [16]. According to this report, the increase in HER efficiency was influenced by better orbital overlap between the carbon atoms in C_{60} and the two hydrogen atoms in the adsorbed water molecule. The result demonstrates that the role of the nanocarbon scaffold in donation/gaining electrons in ORR/OER/HER is just as important as the role of metallic reaction sites.

Electronic properties of carbon nanotubes are determined by their π-electron band structure, which is symmetrical with respect to the charge neutrality point (CNP). In pristine nanotube, density of π-electron states (DOS) at CNP is close or equal to zero in metallic or semiconducting nanotubes, respectively. As we move away from CNP towards lower or higher energies, DOS increases. Thanks to this feature, it is very easy to change the major charge carriers between electrons and holes. Therefore CNTs, like graphene, are classified as ambipolar semiconductors [17]. These characteristics of CNTs allow us to control the concentration of electrons or holes through gating, which is implemented in FETs, or through doping. Doping strategies include: substitutional doping with heteroatoms [18, 19], covalent functionalization [20] and surface doping [21, 22].

We show in this study that acceptor and donor dopants significantly influence the kinetics of heterogeneous electron transfer (HET) between CNTs and electroactive species in electrolyte. We focus on the three electrochemical reactions, ORR, HER and OER, which are particularly interesting in terms of energy conversion technology. The study is limited to the electrode reaction rates, we do not consider the effect of free energy changes for reactants and intermediates.

2. METHODS

DOS of pristine, B-doped, N-doped and -OH functionalized CNT(5,5) was calculated using density functional theory (DFT). As an initial model, nanotube made of 420 carbon atoms was considered. In calculations, the exchange-correlation functional ωB97XD [23] and 6-31G(d) basis set were used, which are a reasonable combination for studying the large organic systems [24]. For numerical simulations, the Gaussian16 computational package was used [25]. To extract the DOS data from from Gaussian output data, we used GaussSum software (Version 3.0, https://gausssum.sourceforge.net/) [26].

Cathodic (anodic) reaction rates, k_c (k_a), have been calculated based on the Gerischer-Marcus integrals [27-29]

$$k_c(E) \propto \int_{-\infty}^{\infty} f(\epsilon - eE)\,\mathrm{DOS}(\epsilon - eE)\,W_{ox}(\epsilon)\,d\epsilon, \quad (1)$$

$$k_a(E) \propto \int_{-\infty}^{\infty} [1 - f(\epsilon - eE)]\,\mathrm{DOS}(\epsilon - eE)\,W_{red}(\epsilon)\,d\epsilon, \quad (2)$$

where E is electrode potential, f (ϵ–eE) is the Fermi-Dirac distribution and

$$W_{\mathrm{ox,red}}(\epsilon) = \frac{1}{4\pi\lambda kT}\exp\left(-\frac{(\epsilon - \epsilon_{\mathrm{F,redox}} \mp \lambda)^2}{4kT\lambda}\right) \quad (3)$$

are Gaussian distributions of electron states of oxidized and reduced form of redox couple in electrolyte. Oxidized and reduced states are located above and below Fermi level of redox species, $\epsilon_{\mathrm{F,redox}}$, respectively, and are separated by doubled reorganization energy, λ. The $\epsilon_{\mathrm{F,redox}}$ is the equivalent of the thermodynamic standard potential of specific electrode reaction, E_0. Standard potentials were converted to the absolute energy scale using the Trassati rule: $\epsilon_{\mathrm{F,redox}}$ [eV] = –4.5 eV – eE (V vs. SHE) [30]. The simulations concerned the following electrode reactions: $O_2 + 2H_2O + 4e^- \rightarrow 4OH^-$ (ORR in alkaline media, E_0 = 0.40 V vs. SHE), $2H^+ + 2e^- \rightarrow H_2$ (HER, E_0 = 0.0 V vs. SHE), $2H_2O \rightarrow O_2(g) + 4H^+ + 4e^-$ (OER, E_0 = 1.23 V vs. SHE). The reorganization energy, λ, was set to 0.5 eV.

The ORR, HER and OER were measured in 0.1 M KOH aqueous solution in three electrode cell connected to a VIONIC potentiostat (Metrohm AG, Switzerland). Linear sweep voltammetry (LSV) measurements were

carried out on glassy carbon rotating disk electrode modified with commercial CNTs and OH–CNTs (Institute of Carbon Technologies Sp. z o.o., Toruń, Poland) at electrode rotation speed of 1600 rpm.

3. RESULTS

Figure 1 shows the positions of the standard redox potentials with respect to the electron states of CNT both in absolute energy and the electrochemical scale. In case of ORR and HER (cathodic reactions) the electron transfer occurs between filled states of CNT, i.e. product of DOS and $f(\epsilon)$, and unoccupied electron states of the oxidized form of redox couple, which are represented by W_{ox}. The reverse process occurs during OER (anodic reaction), where electrons from filled states of the reduced form are transferred to the unoccupied states of CNT, which are represented by product of DOS and $1 - f(\epsilon)$. The applied positive/negative potential E causes a shift of DOS and $f(\epsilon)$ to lower/higher energy.

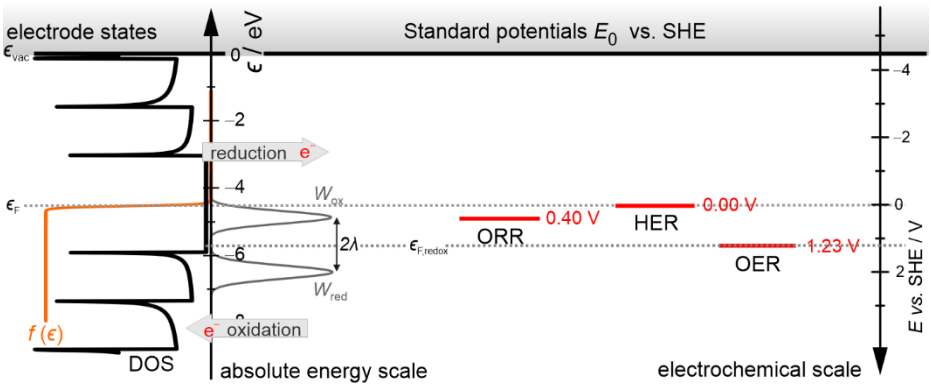

Figure 1 Distribution of electron states of CNT electrode represented by product of DOS and $f(\epsilon)$ and redox species represented by W_{ox} and W_{red}. The positions of the standard potentials for ORR, HER and OER are marked as red horizontal dashes.

3.1 Interstitial doping with B and N

The impact of interstitial doping with boron on DOS is shown in **Figure 2a**. The energy $\epsilon = 0$ corresponds to the ϵ_F. The DOS of the pristine nanotube is approximately symmetrical with respect to the Fermi level. Below and above the Fermi level, local maxima appear, which originate from the van Hove singularities. Valence and conduction bands below and above the ϵ_F are separated by a quasi-band gap with a width of approximately 2 eV. Introduction of boron atoms into the tubule walls in concentration of 0.5 at% results in creation of new states above the edge of the valence band and narrowing of the band gap by about 0.5 eV.

As we show in **Figure 2b and c**, changes in DOS caused by B-doping affect the curves of cathodic reaction rates, k_c. Both in ORR and HER, onset potentials at B-doped CNT is slightly shifted to lower potentials. On the other hand, since lowering the electrode potential causes faster growth in the number of filled electron states participating in electron transfer, the slope of the k_c curve is greater at B-doped CNT electrodes than at pristine CNTs. The curves of the OER rates are much strongly affected by acceptor doping (**Figure 2d**). In this anodic reaction participate unoccupied electronic states of CNTs, which, with increasing electrode potential, are gradually filled with electrons from reduced form of redox pairs. Since the increase in the number of unoccupied states with increasing positive electrode potential is much faster in acceptor-doped nanotubes than in pristine ones, we expect much better anodic reaction performance on boron-doped nanotubes. This is indeed the case. The onset potential on the B-CNT is as much as about 0.4 V lower than on the pristine CNT. Also, the slope of the k_a curve is greater on the B-CNT electrode than on the pristine CNT ones.

We observe the opposite effect when replacing C atoms with N. As a result of N-doping, donor states are formed below the edge of the conduction band, and the quasi-band gap narrows by approximately 0.5 eV

(**Figure 2a**). Acceptor states contribute significantly to the increase in cathode reaction efficiency. For both ORR and HER, the onset potential shifts by about 0.5 V toward less negative electrode potentials. The excess of electron carriers in the donor-doped electrode should hinder the efficiency of the anodic reaction (**Figure 2d**). However, we observe an increase in the slope of the k_a curve on the N-CNT electrode compared to the pristine CNT electrode and an almost unchanged initial reaction potential. This can be easily explained if we consider that unoccupied electron states of the electrode participate in the anodic reaction. Interstitial N-doping creates additional states below the conduction band edge, but does not lead to the disappearance of states just below the upper edge of the valence band. Therefore, the onset of the increase in the number of unoccupied states with increasing electrode potential will be similar for N-CNT and pristine CNT. In turn, the greater slope of the k_a curve on the N-CNT electrode is caused by unoccupied states created by donor doping.

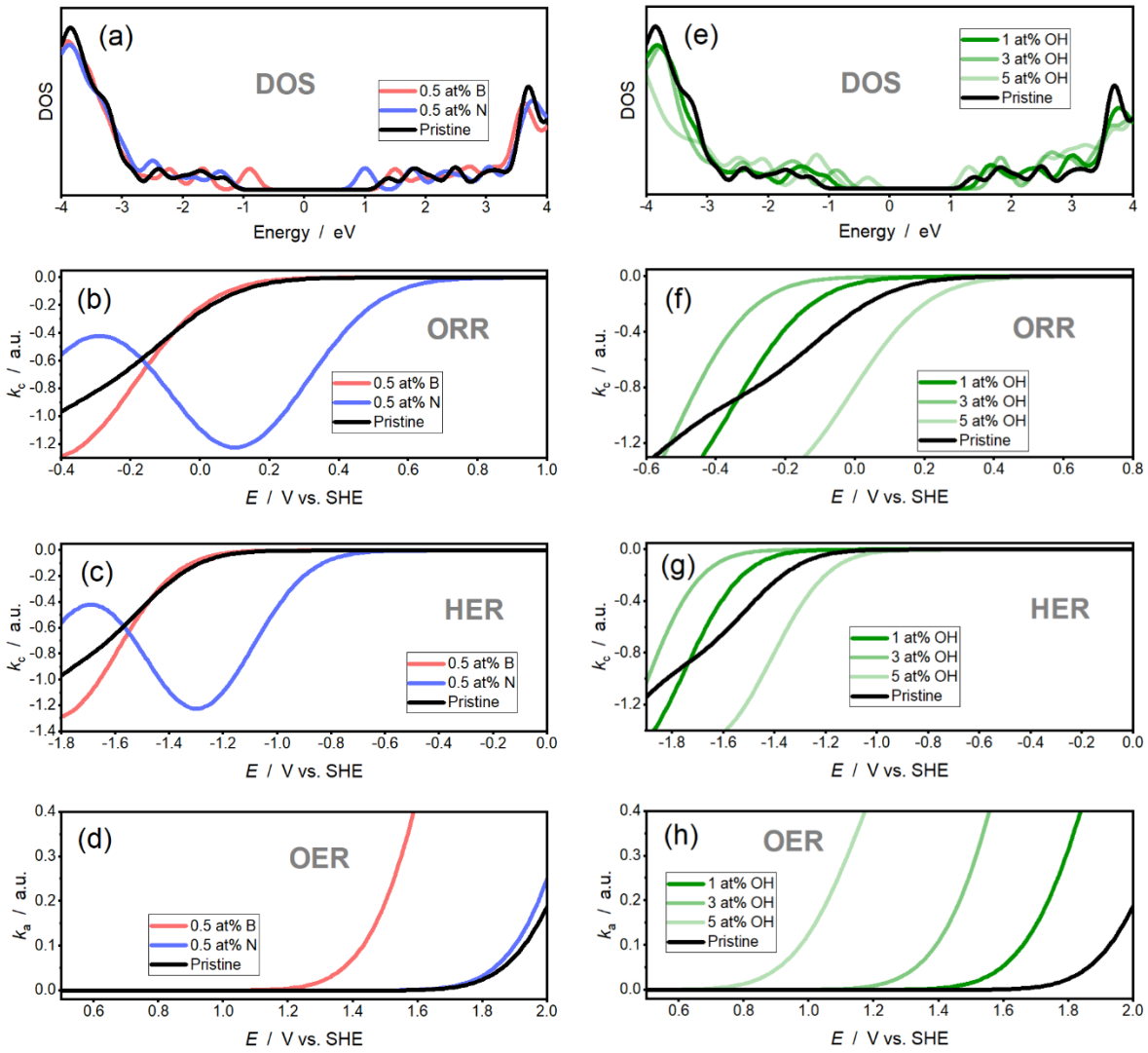

Figure 2 DOS and corresponding electrode reaction rates of ORR, HER and OER. **(a-d)** Boron and nitrogen doped CNTs. **(e-h)** CNTs covalently functionalized with the –OH group.

3.2 Doping by functionalization with -OH group

Effect of hydroxylation on DOS of CNT is shown in **Figure 2e**. In general, covalently attached OH groups act as acceptor dopants, which is a consequence of the direct transfer of electrons from the nanotube to –OH. With increasing concentration of the attached –OH groups, new electronic states are created above the edge of the valence band. At the same time, electronic states above the edge of the conduction band disappear.

However, at higher –OH concentrations (5 at% OH), the narrowing of the quasi-band gap is observed, i.e. new states are also created below the edge of the conduction band of pristine CNT.

The changes of DOS are reflected by changes of reaction rates for ORR and HER, which are shown in **Figure 2f and g**. The k_c curves shift to more negative potentials by 0.1 V and 0.2 V with respect to pristine CNTs at the –OH concentration of 1at% and 3at%, respectively, and the cathodic reaction is impeded. However, at concentration of 5 at%, due to the states created below the edge of the conduction band, the k_c curve shifts by about 0.1 V to the less negative electrode potentials with respect to pristine CNTs, and the cathodic reaction is facilitated. In the anodic OER shown in **Figure 2h**, the k_a curve shifts significantly to less positive electrode potential with increasing –OH concentration. At the –OH concentration of 5 at%, the shift is as much as ~1 V.

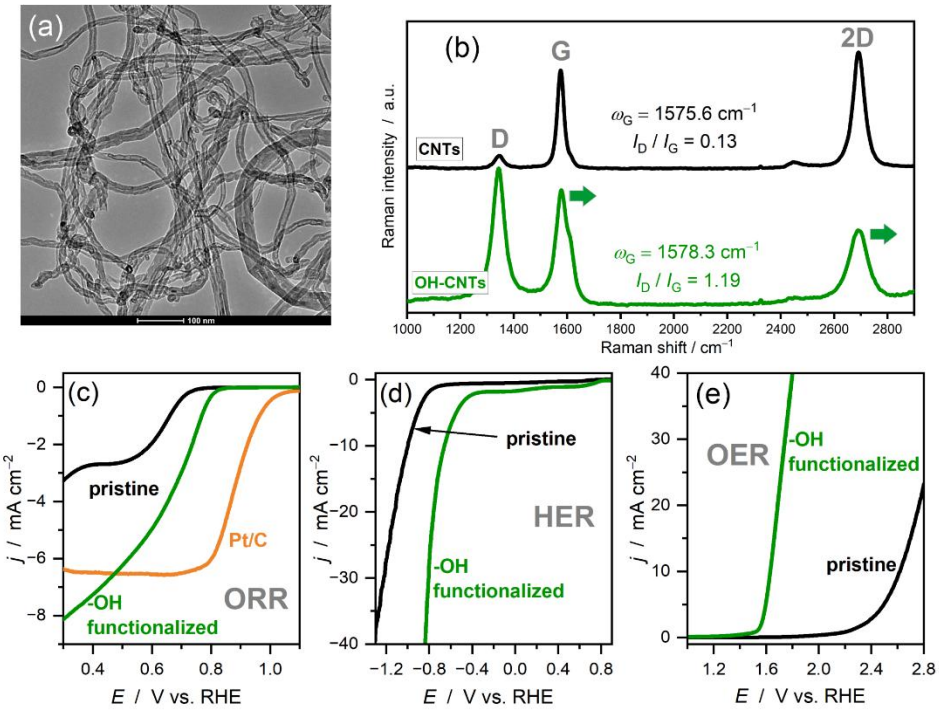

Figure 3 (a) TEM image of the examined OH-CNTs. **(b)** Raman spectra of pristine and -OH functionalized carbon nanotubes. **(c)** LSV curves of ORR measured in O_2 saturated 0.1 M KOH aqueous solution at RDE speed of 1600 rpm. **(d)** and **(e)** LSV curves of HER and OER in N_2 purged 0.1 M KOH aqueous solution at RDE speed of 1600 rpm.

To assess the extent to which the presented calculations reflect realistic physical systems, measurements of ORR, HER, and OER were performed on commercial pristine and –OH functionalized multiwalled CNTs shown in **Figure 3a**. Functionalization causes changes in the position and intensity of the main Raman features, which are shown in **Figure 3b**. The relative intensity of the defect induced D band in the Raman spectrum increases in the –OH functionalized CNTs [31]. The doping effect caused by functionalization is reflected by the shift of the Raman G and 2D bands to higher wave numbers by 2.7 and 3.5 cm^{-1}, respectively. In **Figure 3c**, we show the LSV curves for ORR recorded in 0.1 M KOH aqueous solution. The onset potential for ORR at the hydroxylated CNT electrode is shifted to less negative potential by ~0.1 V with respect to the pristine CNT electrode. A greater slope of the ORR curve was also observed on the OH-CNT electrode than on pristine CNT. These results are consistent with the model predictions for nanotubes with an –OH group concentration of 5 at%. HER measurements shown in **Figure 3d** give similar results. A significant shift of the onset potential of cathodic reaction to less negative electrode potentials and an increase in the slope of the $j(E)$ curve at OH-CNT electrode with respect to the pristine CNT are also observed. LSV data for OER shown in **Figure 3e** are

consistent with calculations as well. The onset potential for OER at the OH-CNT electrode is shifted to lower potentials by as much as ~0.8 V with respect to the pristine CNTs. The increased slope of the $j(E)$ curve on the OH-CNT electrode is also apparent.

4. CONCLUSION

We have shown that CNTs, despite low catalytic activity compared to intensively studied transition metal oxides and alloys, are good benchmark system for studying of the doping effect on catalysis of ORR, HER and OER. Simulations based on the Gerischer-Marcus model show that donor doping caused by substitution of carbon atoms with N atoms results in reduction of overpotential for ORR and HER (cathodic reactions) and increasing of the slope of $k_c(E)$ curve. A similar phenomenon, i.e. reduction of overpotential for OER (anodic reaction) and increasing of the slope of $k_a(E)$ curve, is caused by introduction of acceptor dopant (boron) into nanotube walls. In summary, donor doping facilitates cathodic reactions, while acceptor doping facilitates anodic reactions. The acceptor doping effect can be also achieved by hydroxylation of nanotubes. Simulations show that at –OH concentrations of 1at% and 3at%, the cathodic ORR and HER are hindered, while the efficiency of the anodic OER significantly increases. At sufficiently high –OH concentration of 5at%, both cathodic and anodic reactions are facilitated. The predictions of the Gerischer-Marcus model have been experimentally confirmed for hydroxylated CNTs.

ACKNOWLEDGEMENTS

The research was partially funded by the Ministry of Science and Higher Education under the program 'Regional Initiative of Excellence' in years 2024–2027, Project No. RID/SP/0048/2024/01.

REFERENCES

[1] AKBARI, E.,BUNTAT, Z., Benefits of using carbon nanotubes in fuel cells: a review. *International Journal of Energy Research*. 2017, vol. 41, no. 1, pp. 92-102.

[2] DETHAN, J.F.,SWAMY, V., Mechanical and thermal properties of carbon nanotubes and boron nitride nanotubes for fuel cells and hydrogen storage applications: A comparative review of molecular dynamics studies. *International Journal of Hydrogen Energy*. 2022, vol. 47, no. 59, pp. 24916-24944.

[3] LAWAL, A.T., Recent application of carbon nanotubes in energy storage and conversion devices. *Carbon Trends*. 2025, vol. 19, 100470.

[4] WEI, P., LI, X., HE, Z., SUN, X., et al., Porous N, B co-doped carbon nanotubes as efficient metal-free electrocatalysts for ORR and Zn-air batteries. *Chemical Engineering Journal*. 2021, vol. 422, 130134.

[5] BÉJAR, J., ESPINOSA–MAGAÑA, F., AVELAR, J., AGUILAR–ELGUEZABAL, A., et al., Rational design of nitrogen–doped carbon nanotubes by defect engineering for Zn–air batteries with high performance. *Carbon*. 2023, vol. 204, pp. 411-426.

[6] ZHU, S., SHENG, J., CHEN, Y., NI, J., et al., Carbon nanotubes for flexible batteries: recent progress and future perspective. *National Science Review*. 2021, vol. 8, no. 5, nwaa261.

[7] TOMA, F.M., SARTOREL, A., IURLO, M., CARRARO, M., et al., Tailored functionalization of carbon nanotubes for electrocatalytic water splitting and sustainable energy applications. *ChemSusChem*. 2011, vol. 4, no. 10, pp. 1447.

[8] CHENG, Y., XU, C., JIA, L., GALE, J.D., et al., Pristine carbon nanotubes as non-metal electrocatalysts for oxygen evolution reaction of water splitting. *Applied Catalysis B: Environmental*. 2015, vol. 163: pp. 96-104.

[9] LIN, L., MA, Y., ZETTSU, N., VEQUIZO, J.J.M., et al., Carbon nanotubes as a solid-state electron mediator for visible-light-driven Z-scheme overall water splitting. *Journal of the American Chemical Society*. 2024, vol. 146, no. 21, pp. 14829-14834.

[10] ALI, A., MUQADDAS, S., ALDOSARI, H., RASHID, S., et al., Novel structured carbon nanotubes fiber based microelectrodes for efficient electrochemical water splitting and glucose sensing. *Carbon*. 2024, vol. 218, 118709.

[11] HUANG, C., WANG, F., CHEN, X., LI, J., et al., Innovative strategies for designing and constructing efficient fuel cell electrocatalysts. *Chemical Communications*. 2025.

[12] XIE, W., ZHU, K., YANG, H.,YANG, W., Advancements in achieving high reversibility of zinc anode for alkaline zinc-based batteries. *Advanced Materials*. 2024, vol. 36, no. 5, 2306154.

[13] ZHANG, X., LIU, Y., ZHAO, X., CHENG, Z., et al., Recent advances and perspectives of high-entropy alloys as electrocatalysts for metal-air batteries. *Energy & Fuels*. 2024, vol. 38, no. 20, pp. 19236-19252.

[14] YAO, Y., LI, Z., DOU, Y., JIANG, T., et al., High entropy alloy nanoparticles encapsulated in graphitised hollow carbon tubes for oxygen reduction electrocatalysis. *Dalton Transactions*. 2023, vol. 52, no. 13, pp. 4142-4151.

[15] SUN, H., XU, X., KIM, H., SHAO, Z., et al., Advanced electrocatalysts with unusual active sites for electrochemical water splitting. *InfoMat*. 2024, vol. 6, no. 1, e12494.

[16] HOU, G.L., YANG, T., LI, M., VANBUEL, J., et al., Water splitting by C60-supported vanadium single atoms. *Angewandte Chemie International Edition*. 2021, vol. 60, no. 52, pp. 27095-27101.

[17] HU, W., SHENG, Z., HOU, X., CHEN, H., et al., Ambipolar 2D semiconductors and emerging device applications. *Small Methods*. 2021, vol. 5, no. 1, 2000837.

[18] LIU, Y., SHEN, Y., SUN, L., LI, J., et al., Elemental superdoping of graphene and carbon nanotubes. *Nature communications*. 2016, vol. 7, no. 1, 10921.

[19] HA, S., CHOI, G.B., HONG, S., KIM, D.W., et al., Substitutional boron doping of carbon materials. *Carbon letters*. 2018, vol. 27, pp. 1-11.

[20] BEKYAROVA, E., SARKAR, S., WANG, F., ITKIS, M.E., et al., Effect of covalent chemistry on the electronic structure and properties of carbon nanotubes and graphene. *Accounts of chemical research*. 2013, vol. 46, no. 1, pp. 65-76.

[21] HU, T.,GERBER, I.C., Theoretical study of the interaction of electron donor and acceptor molecules with graphene. *The Journal of Physical Chemistry C*. 2013, vol. 117, no. 5, pp. 2411-2420.

[22] SZROEDER, P., ZIÓŁKOWSKI, P., MOSIŃSKA, L.,TRYKOWSKI, G., Boosting electrochemical performance of single-walled carbon nanotube three-dimensional architectures through appropriate selection of organic dispersant. *Diamond and Related Materials*. 2024, vol. 148, 111440.

[23] CHAI, J.-D.,HEAD-GORDON, M., Long-range corrected hybrid density functionals with damped atom–atom dispersion corrections. *Physical Chemistry Chemical Physics*. 2008, vol. 10, no. 44, pp. 6615-6620.

[24] SAHALIANOV, I., HYNYNEN, J., BARLOW, S., MARDER, S.R., et al., UV-to-IR absorption of molecularly p-doped polythiophenes with alkyl and oligoether side chains: Experiment and interpretation based on density functional theory. *The Journal of Physical Chemistry B*. 2020, vol. 124, no. 49, pp. 11280-11293.

[25] FRISCH, M., TRUCKS, G., SCHLEGEL, H., SCUSERIA, G., et al., Gaussian 16 Revision C. 01, 2016. *Gaussian Inc. Wallingford CT*. 2016, vol. 1: pp. 572.

[26] O'BOYLE, N.M., TENDERHOLT, A.L.,LANGNER, K.M., Cclib: a library for package-independent computational chemistry algorithms. *Journal of computational chemistry*. 2008, vol. 29, no. 5, pp. 839-845.

[27] GERISCHER, H., Über den Ablauf von Redoxreaktionen an Metallen und an Halbleitern. *Zeitschrift für Physikalische Chemie*. 1960, vol. 26, no. 3_4, pp. 223-247.

[28] HELLER, I., KONG, J., HEERING, H.A., WILLIAMS, K.A., et al., Individual single-walled carbon nanotubes as nanoelectrodes for electrochemistry. *Nano Letters*. 2005, vol. 5, no. 1, pp. 137-142.

[29] SZROEDER, P., BANASZAK-PIECHOWSKA, A.,SAHALIANOV, I., Tailoring Electrocatalytic Properties of sp2-Bonded Carbon Nanoforms Through Doping. *Molecules*. 2025, vol. 30, no. 6, pp. 1265.

[30] TRASATTI, S., The absolute electrode potential: an explanatory note (Recommendations 1986). *Pure and Applied Chemistry*. 1986, vol. 58, no. 7, pp. 955-966.

[31] SZROEDER, P., ZIÓŁKOWSKI, P., SAHALIANOV, I., MADAJSKI, P., et al., The Hydroxylated Carbon Nanotubes as the Hole Oxidation System in Electrocatalysis. *Materials*. 2024, vol. 17, no. 14, 3532.